

IMMUNOBIOLOGY AND IMMUNOTHERAPY

Selective homing of CAR-CIK cells to the bone marrow niche enhances control of the acute myeloid leukemia burden

Marta Biondi,^{1,2} Sarah Tettamanti,¹ Stefania Galimberti,³ Beatrice Cerina,¹ Chiara Tomasoni,¹ Rocco Piazza,^{2,4} Samantha Donsante,⁵ Simone Bido,⁶ Vincenzo Maria Perriello,⁷ Vania Broccoli,^{6,8} Andrea Doni,⁹ Francesco Dazzi,¹⁰ Alberto Mantovani,^{9,11,12} Gianpietro Dotti,¹³ Andrea Biondi,^{2,14} Alice Pievani,^{1,*} and Marta Serafini^{1,*}

¹Tettamanti Center, Fondazione IRCCS San Gerardo dei Tintori, Monza, Italy; ²Department of Medicine and Surgery and ³Bicocca Bioinformatics Biostatistics and Bioimaging B4 Center, School of Medicine and Surgery, University of Milano-Bicocca, Monza, Italy; ⁴Hematology, Fondazione IRCCS San Gerardo dei Tintori, Monza, Italy; ⁵Department of Molecular Medicine, Sapienza University, Rome, Italy; ⁶Division of Neuroscience, San Raffaele Scientific Institute, Milan, Italy; ⁷Institute of Hematology, University and Hospital of Perugia, Perugia, Italy; ⁸National Research Council (CNR), Institute of Neuroscience, Milan, Italy; ⁹Unit of Advanced Optical Microscopy, IRCCS Humanitas Research Hospital, Rozzano, Milan, Italy; ¹⁰School of Cardiovascular Sciences, King's College London, London, United Kingdom; ¹¹Department of Biomedical Sciences, Humanitas University, Pieve Emanuele, Milan, Italy; ¹²William Harvey Research Institute, Queen Mary University, London, United Kingdom; ¹³Lineberger Comprehensive Cancer Center, University of North Carolina, Chapel Hill, NC; and ¹⁴Pediatrics, Fondazione IRCCS San Gerardo dei Tintori, Monza, Italy

KEY POINTS

- CAR T-cell therapy in AML is hampered by the poor accumulation of effector cells in the BM niche in which leukemic stem cells are nested.
- Engineering CAR-CIKs with CXCR4 promotes their homing in the BM and improves their antileukemic efficacy in AML.

Acute myeloid leukemia (AML) is a hematological malignancy derived from neoplastic myeloid progenitor cells characterized by abnormal clonal proliferation and differentiation. Although novel therapeutic strategies have recently been introduced, the prognosis of AML is still unsatisfactory. So far, the efficacy of chimeric antigen receptor (CAR)-T-cell therapy in AML has been hampered by several factors, including the poor accumulation of the blood-injected cells in the leukemia bone marrow (BM) niche in which chemotherapy-resistant leukemic stem cells reside. Thus, we hypothesized that overexpression of CXCR4, whose ligand CXCL12 is highly expressed by BM stromal cells within this niche, could improve T-cell homing to the BM and consequently enhance their intimate contact with BM-resident AML cells, facilitating disease eradication. Specifically, we engineered conventional CD33.CAR-cytokine-induced killer cells (CIKs) with the wild-type (wt) CXCR4 and the variant CXCR4^{R334X}, responsible for leukocyte sequestration in the BM of patients with warts, hypogammaglobulinemia, immunodeficiency, and myelokathexis syndrome. Overexpression of both CXCR4^{wt} and CXCR4^{mut} in CD33.CAR-CIKs resulted in

significant improvement of chemotaxis toward recombinant CXCL12 or BM stromal cell-conditioned medium, with no observed impairment of cytotoxic potential in vitro. Moreover, CXCR4-overexpressing CD33.CAR-CIKs showed enhanced in vivo BM homing, associated with a prolonged retention for the CXCR4^{R334X} variant. However, only CD33.CAR-CIKs coexpressing CXCR4^{wt} but not CXCR4^{mut} exerted a more sustained in vivo antileukemic activity and extended animal survival, suggesting a noncanonical role for CXCR4 in modulating CAR-CIK functions independent of BM homing. Taken together, these data suggest that arming CAR-CIKs with CXCR4 may represent a promising strategy for increasing their therapeutic potential for AML.

Introduction

The therapeutic potential of chimeric antigen receptor (CAR) T cells for patients with acute myeloid leukemia (AML) is still far from being realized because of multiple hurdles. The main obstacles include the lack of leukemic stem cells (LSCs)/AML-specific target antigens, the disease heterogeneity, and the leukemia-induced remodeling of the bone marrow (BM) microenvironment. So far, efforts to potentiate CAR T-cell

therapy in AML have mostly focused on identifying optimal antigens and CAR structures to promote more specific targeting and on counteracting the leukemia-induced immune suppression via combination therapy using immune checkpoint blocking antibodies.¹

However, fundamental to the optimization of CAR T-cell clinical outcome is also the requirement for blood-injected cells to efficiently reach and persist at the tumor site. Such a challenge,

well documented in solid tumors, has, in the last few years, extended to hematological malignancies in which the BM is the primary location for acute leukemia initiation, maintenance, progression, and chemoresistance. This is mainly relevant in the AML context because innovative curative treatments must have the potential to eliminate LSCs that reside in the BM niche in which they persist after conventional treatments. Accumulating evidence suggests that CAR T-cell homing ability to the BM microenvironment is a prerequisite to mediate consistent therapeutic activity in AML.

For instance, a small data set from a phase 1 clinical study with anti-Lewis (Le)-Y.CAR T cells seems to suggest that the accumulation of CAR T cells in the BM correlates with better clinical outcome, supporting the hypothesis that improving T-cell trafficking to the BM may increase their therapeutic effects.²

Chemokines and their receptors play a crucial role in the migration and homing of lymphocytes. A key requirement for efficient migration of cytotoxic T cells is that they express chemokine receptors that match the chemokines produced by tumor or tumor-associated cells. However, culture conditions for the expansion of human lymphocytes dampen the expression of chemokine receptors and may negatively influence their homing ability to the BM.^{3,4} Therefore, CAR T cells may be modified to express chemokine receptors to potentiate their migratory and infiltrative capacity. Notably, this approach has shown promising results in numerous preclinical tumor models.⁵⁻⁹ Furthermore, there are some ongoing clinical trials using chemokine receptors CCR4 (NCT03602157) and CXCR4 (NCT04727008) to improve CAR T cells trafficking to the tumor site.

Trafficking of lymphocytes into the BM relies on the expression of CXCR4, a chemokine receptor that binds to the chemokine CXCL12, which is highly expressed by stromal and endothelial cells in the BM. Specifically, in AML, blasts overexpressing CXCR4 interact with CXCL12, improving their homing to the protective BM microenvironment and their exposure to pro-survival signals.¹⁰ The CXCL12/CXCR4 interaction keeps leukemic blasts in close contact with supporting stromal cells and the extracellular matrix constitutively releasing growth-promoting and antiapoptotic signals that contribute to AML immune escape. Furthermore, blocking the CXCL12/CXCR4 interaction with the inhibitor plerixafor disrupts AML blast interaction with the BM microenvironment, causing AML cell mobilization into the circulation.^{11,12}

We tested the hypothesis that previously optimized CD33.CAR-cytokine-induced killer cells (CIKs), which are ex vivo expanded T lymphocytes with a mixed T-natural killer (NK) phenotype endowed with MHC-unrestricted antitumor activity,¹³ overexpressing CXCR4 would acquire superior homing ability to the BM and, therefore, enhanced elimination of BM-resident AML cells. Furthermore, we also tested whether increasing CD33.CAR-CIKs retention in the BM via the coexpression of the CXCR4 gain-of-function (GOF) variant (R334X mutation) described in the warts, hypogammaglobulinemia, immunodeficiency, and myelokathexis (WHIM) syndrome would further increase the antitumor effects of CD33.CAR-CIKs.¹⁴ R334X mutation causes a carboxyl-terminal truncation, which impairs CXCR4 internalization upon CXCL12 binding and therefore

results in increased receptor signaling compared with the wild-type (wt) counterpart.¹⁵

Materials and methods

Generation of CAR constructs

Three bicistronic Sleeping Beauty (SB)-transposon vectors were generated by modifying the SB-pT4 CD33-CH3-CD28-OX40- ζ CAR construct (hereafter named CD33.CAR) to encode both human CXCR4 and CD33.CAR: (1) CXCR4(I)CD33.CAR construct, in which both CD33.CAR and CXCR4 expression is driven by an internal ribosome entry site (IRES); and (2) CD33.CAR(2A)CXCR4^{wt} and (3) CD33.CAR(2A)CXCR4^{mut}, in which the CXCR4 coding sequence, in its wt or R334X-mutated form, is cloned downstream to the CD33.CAR sequence linked with self-cleaving peptide 2A.

CIKs differentiation and modification

CAR-CIKs were generated as previously described,^{13,16} by sequentially adding interferon gamma (IFN- γ ; 1000 U/mL; Dompè Biotec) at day 0 and interleukin-2 (IL-2; 300 U/mL; Chiron BV) and anti-CD3 monoclonal antibody OKT3 (50 ng/mL; Janssen-Cilag) at day 1 to peripheral blood mononuclear cells (PBMCs). At the end of the differentiation protocol, mature CIKs typically are almost entirely CD3⁺ T lymphocytes expressing CD8 and CD56 and displaying an effector memory phenotype. For nonviral CIKs modification, the SB-pT4 vector and SB100X transposase were provided by Z. Izsvak (Max-Delbrück-Center for Molecular Medicine, Berlin, Germany).

Transwell migration assay

CAR⁺-CIK migration ability was assessed using 5 μ m-pore 24-transwell plates (Corning). Advanced RPMI 1640 medium (600 μ L) with 2% fetal bovine serum containing 200 ng/mL human recombinant (rh) CXCL12 (Peprotech) was added to the lower chamber, and the upper chamber was filled with 100 μ L of medium containing control CD33.CAR⁻ or CXCR4-overexpressing CD33.CAR⁺-CIKs (0.5×10^6 cells). After 2 hours of incubation, cells of the lower chamber were collected, and after adding 10 μ L of CountBright Absolute Counting Beads (Thermo Fisher Scientific) per tube, the number of migrated cells was quantified via fluorescence-activated cell sorting (FACS).

The same procedure was also followed using supernatants of mesenchymal stromal cells from either healthy donors (HD-MSCs) or pediatric patients with AML (AML-MSCs; supplemental Methods, available on the *Blood* website) as stimuli. CXCR4 blocking was achieved by pretreating CAR⁺-CIKs with 100 μ M plerixafor (Mozobil, Sanofi Oncology) for 30 minutes at 37°C before plating the migration assay. To test the capacity of CXCR4-overexpressing CD33.CAR⁺-CIKs to migrate toward murine CXCL12, 200 ng/mL mouse recombinant CXCL12 (Peprotech) or mouse BM supernatant were used as stimuli.

Conjugated stability assay

KG-1 cells or KG-1 CRISPR CRISPR-associated protein (Cas) 9 CD33 knockout cells (see supplemental Methods), were labeled with Cell Tracer Violet (Thermo Fisher Scientific) and incubated for 30 minutes at 37°C with CD33.CAR⁺-, CD33.CAR⁺-CXCR4^{wt}-, or CD33.CAR⁺-CXCR4^{mut}-CIKs at a

ratio of 1:1 to form conjugates. After this incubation, cells were allowed to migrate through 5 pore to 200 ng/mL rhCXCL12 for 2 hours before FACS analysis.

In vitro CAR-related functional assays

CAR-CIK in vitro effector functions were tested against the CD33⁺ KG-1 cell line or primary AML cells via cytotoxicity, cytokine production, and proliferation assays, both in the presence and absence of rhCXCL12 (see supplemental Methods). Primary AML cells were obtained from the BM and PBMCs collected from patients with AML, after written informed consent was obtained from patients or parents/legal guardians in accordance with the Declaration of Helsinki.

In vivo homing assay

The study was approved by the Italian Ministry of Health. Procedures involving animals conformed with protocols approved by the Milano-Bicocca University in compliance with national and international law and policies. Six- to eight-week-old male NSG (NOD.Cg-Prkdc^{scid}Il2rg^{tm1Wjl}/SzJ) mice (Charles River Laboratories) were sublethally irradiated (200 cGy) 48 hours before treatment with CAR-CIKs. Then, 10⁷ sorted CD33.CAR⁺-CXCR4^{wt}-, CD33.CAR⁺-CXCR4^{mut}-, or control CD33.CAR⁺-CIKs were IV infused. Mice were euthanized from 7 to 14 days after infusion, and the peripheral blood (PB), lungs, spleen, and BM were analyzed via FACS to assess CAR-CIKs engraftment.

In vivo antileukemic activity

NSG mice were IV injected with CD33⁺ KG-1 cells (5 × 10⁶ cells per mouse). Two weeks later, mice were left untreated or infused with 10⁷ sorted CD33.CAR⁺-CXCR4^{wt}-, CD33.CAR⁺-CXCR4^{mut}-, or control CD33.CAR⁺-CIKs.

For end point experiments, mice were euthanized 25 days after CAR-CIK infusion, and PB, spleen, and BM were analyzed via FACS and immunohistochemistry to establish the AML burden (see supplemental Methods).

For survival experiments, AML burden was monitored via BM aspiration and analyzed via FACS at the indicated time points.

Results

CXCR4 expression drops during CAR-CIKs expansion and can be stably restored using bicistronic SB transposon vectors without phenotypic alterations

The CXCL12/CXCR4 axis influences AML LSC nesting into the protective BM niche.¹⁰ We examined bulk RNA sequencing (RNA-seq) data sets obtained from patients with AML available on the The Cancer Genome Atlas database, and confirmed that CXCR4 is highly expressed by AML blasts (n = 173) as compared with healthy PBMCs (n = 70; padj = 7.73e-26; supplemental Figure 1A). Furthermore, analysis of 2 published single-cell RNA-seq data sets from AML BM (EGAS00001005593¹⁷; GSE214914) revealed that CXCR4 expression decreases during myeloid cell maturation (supplemental Figure 1B-C), and it is particularly high on immature cell subsets (>10th percentile on hematopoietic stem cells/multipotent progenitor cells, common myeloid progenitor cells, and granulocyte macrophage progenitor cells)

(supplemental Figure 1D-E). In addition, a single-cell RNA-seq data set of murine BM (GSE128423¹⁸) indicates that CXCL12 is strongly expressed by the BM stromal cells of the MLL-AF9 leukemia model (supplemental Figure 1F-H). We corroborated these data, showing the presence of high levels of CXCL12 in the serum collected from BM samples of patients with AML, which is comparable with levels observed in healthy controls (P = .3011; supplemental Figure 1I).

Because ex vivo culturing of human lymphocytes can affect the expression of chemokine receptors, we analyzed the expression of CXCR4 in CIKs engineered to express the CD33.CAR.¹³ We consistently observed that CD33.CAR-CIKs displayed a significant reduction in CXCR4 expression at the end of culture compared with freshly isolated T cells (n = 16; P < .0001; Figure 1A) in both CD4⁺ and CD8⁺ subpopulations (Figure 1B). This observation, consistent with a previous study,¹⁹ suggests that ex vivo expansion reduces the potential ability of CD33.CAR-CIKs to use the CXCL12 gradient to migrate to the BM after adoptive transfer in patients. Thus, we explored whether CXCR4 overexpression obtained via gene transfer could restore CD33.CAR-CIKs homing to the BM.

Therefore, we designed 2 different bicistronic SB transposon vectors containing either IRES or 2A-like peptide, hereafter named CXCR4(I)CD33.CAR and CD33.CAR(2A)CXCR4 constructs, respectively, to coexpress 2 transgenes under the control of a single promoter (supplemental Figure 2A). The monocistronic CD33.CAR construct was used as a control. The expression of CXCR4 and CD33.CAR was assessed via FACS analysis at the end of 3 weeks of culture (supplemental Figure 2B). CIKs transduced with either CD33.CAR(I)CXCR4 (n = 8) or CXCR4(2A)CD33.CAR (n = 8) vectors showed significantly higher expression of CXCR4 compared with CIKs transduced with the CD33.CAR construct alone (n = 12; P = .0005; supplemental Figure 2C). Notably, we observed that CD33.CAR expression in CIKs transduced with the CD33.CAR(2A)CXCR4 was similar or even higher than that of CIKs transduced with the CD33.CAR construct (P = .028). In contrast, CIKs engineered with the CXCR4(I)CD33.CAR, in which CAR expression is under the control of the IRES element, showed reduced CAR expression compared with CIKs transduced with the CD33.CAR construct (P = .028; supplemental Figure 2D). Accordingly, we selected the 2A peptide-based bicistronic construct to proceed with further investigations.

Several studies have shown that carboxyl-terminal-truncated forms of the CXCR4 receptor, usually expressed on leukocytes of patients with WHIM syndrome, have improved chemotaxis responsiveness toward CXCL12.²⁰ Therefore, we postulated that the transduction of CD33.CAR-CIKs with the most common mutated version of CXCR4 (CXCR4^{mut}) in patients with WHIM syndrome, namely the R334X mutant,²¹ might not only increase the efficiency of BM trafficking but might also promote CAR-CIK retention within the BM niche. We thus developed an alternative 2A peptide-based bicistronic SB transposon vector to mediate the coexpression of CD33.CAR and CXCR4^{mut} (Figure 1C). Transfection of CIKs with both bicistronic vectors resulted in an increased and stable CXCR4 expression compared with CD33.CAR-CIKs (Figure 1C-D). Specifically, CD33.CAR-CXCR4^{mut}-CIKs (n = 19) displayed consistent increase of CXCR4 MFI compared with both CD33.CAR-CIKs

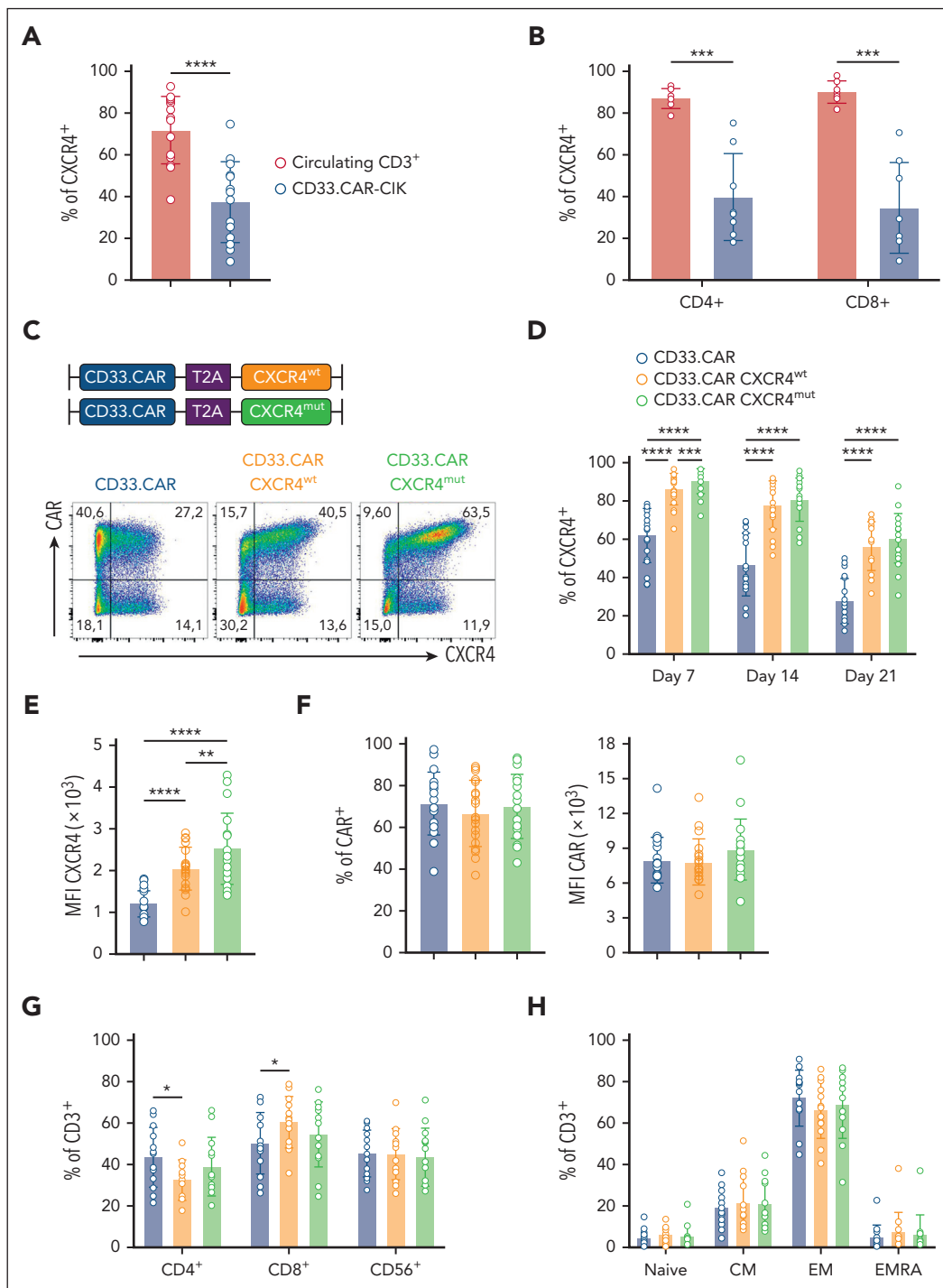


Figure 1. Ex vivo expansion of CD33.CAR-CIKs is associated with downregulation of CXCR4, and its expression can be stably increased using bicistronic SB transposon vectors without phenotypic alterations. Data are presented as individual values and the mean \pm standard deviation (SD). (A-B) Summary of the percentage of CXCR4 expression on circulating CD3⁺ T cells and on CD33.CAR-CIKs at the end of ex vivo expansion. The analysis was performed on (A) all CD3⁺ cells (n = 16 different donors; ****P < .0001 using paired t test) and on (B) CD4⁺ and CD8⁺ subpopulations (n = 8 different donors; ***P = .0003 for CD4⁺; and ***P = .00011 for CD8⁺, using t test). (C) Schematic representation of the vectors encoding CD33.CAR and CXCR4^{wt} or CXCR4^{mut}. Representative flow cytometry plots showing CD33.CAR and CXCR4 expression in CIKs transduced with CD33.CAR, CD33.CAR(2A)CXCR4^{wt}, or CD33.CAR(2A)CXCR4^{mut} transposon vectors. (D-E) Summaries of CXCR4 expression percentage in culture during time (D) and of CXCR4 mean fluorescence intensity (MFI) at the end of the culture (E) on CD33.CAR-, CD33.CAR-CXCR4^{wt}-, and CD33.CAR-CXCR4^{mut}-CIKs (n = 19 different donors; ****P < .0001; ***P = .0003; **P = .0012, using paired t test). (F) Summary of CD33.CAR expression percentage (left) and MFI (right) on CD33.CAR-, CD33.CAR-CXCR4^{wt}-, and CD33.CAR-CXCR4^{mut}-CIKs after ex vivo expansion (n = 19 different donors). (G) Percentages of CD4⁺, CD8⁺, CD56⁺ cells on CD3⁺ for CD33.CAR-, CD33.CAR-CXCR4^{wt}-, and CD33.CAR-CXCR4^{mut}-CIKs after ex vivo expansion (n = 13 different donors; *P = .015 for CD4⁺; and *P = .031 for CD8⁺, using paired t test). (H) Different memory cell subsets (naive, central memory [CM], effector memory [EM], and effector memory reexpressing CD45RA [EMRA] cells) on CD3⁺ for CD33.CAR-, CD33.CAR-CXCR4^{wt}-, and CD33.CAR-CXCR4^{mut}-CIKs after ex vivo expansion (n = 13 different donors).

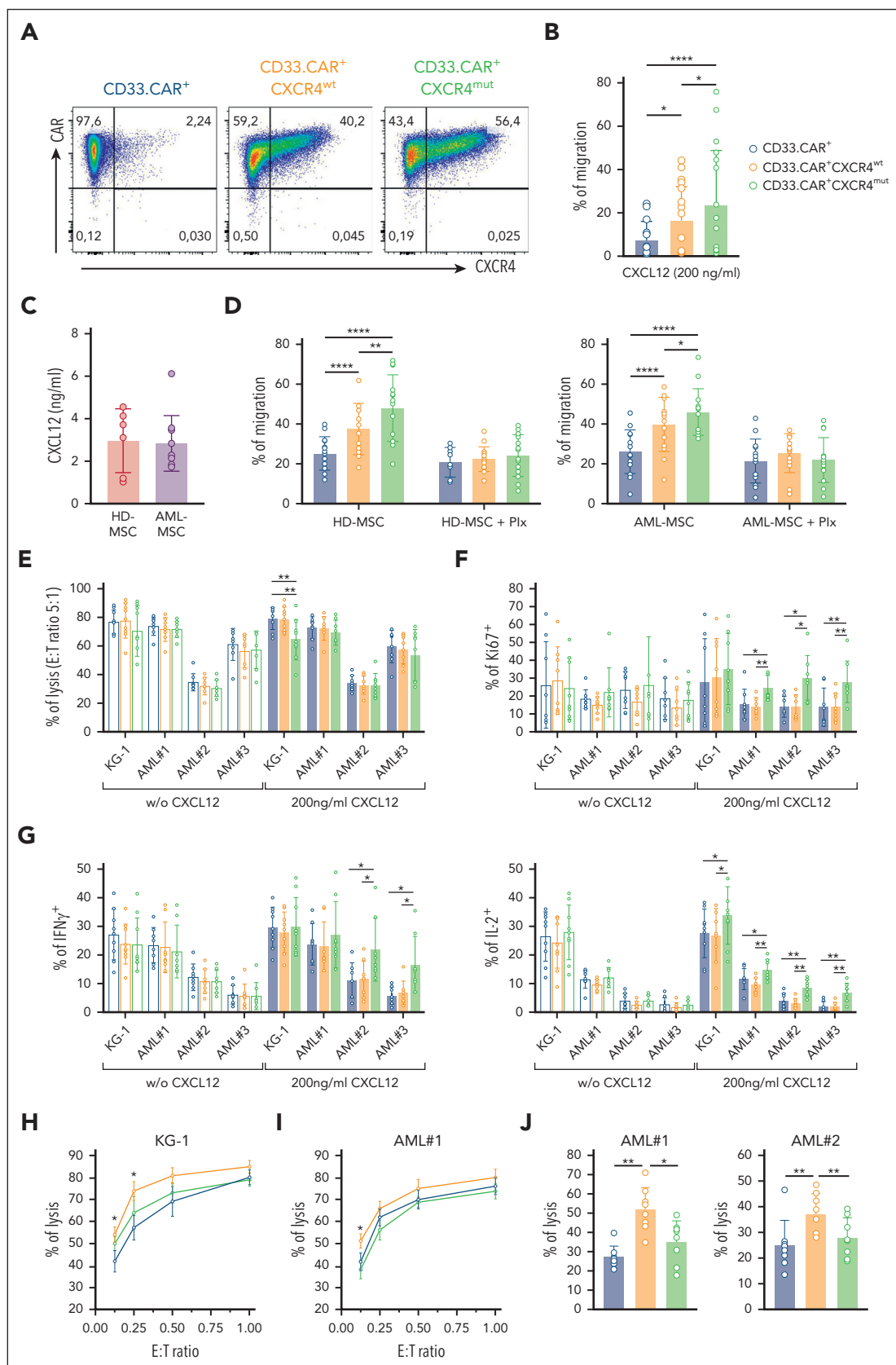


Figure 2. CXCR4-overexpressing CD33.CAR-CIKs have improved migration capability toward CXCL12 and retain antitumor activity in vitro. Data are presented as individual values and the mean \pm SD. (A) Representative flow cytometry plots showing CD33.CAR and CXCR4 expression on purified CD33.CAR⁺, CD33.CAR⁺-CXCR4^{wt}, and CD33.CAR⁺-CXCR4^{mut}-CIKs (supplemental Methods). (B) Percentage of migration of CXCR4-overexpressing CD33.CAR-CIKs in response to CXCL12 in transwell assays (n = 10 independent experiments using CAR-CIKs generated from 10 different donors; ****P < .00001; *P = .015 for CD33.CAR⁺- vs CD33.CAR⁺-CXCR4^{wt}-CIKs; *P = .0362 for CD33.CAR⁺-CXCR4^{wt} vs CD33.CAR⁺-CXCR4^{mut}-CIKs).

($P < .0001$) and CD33.CAR-CXCR4^{wt}-CIKs ($P = .0012$) at the end of the culture period (Figure 1E). CD33.CAR expression was equally maintained among the 3 different constructs ($n = 19$; Figure 1F). CD33.CAR-CIKs expressing either CXCR4^{wt} or CXCR4^{mut} retained the expression of typical phenotypic markers (CD4, CD8, CD56, CD45RO, and CD62L), with a slight alteration in CD4⁺ and CD8⁺ subsets in CD33.CAR-CXCR4^{wt}- compared with CD33.CAR-CIKs (Figure 1G). No differences were observed in the memory phenotype (Figure 1H).

CXCR4 R334X GOF mutation is associated with decreased receptor internalization and enhanced surface recovery of its expression after protracted CXCL12-induced activation.^{20,22} We observed that CD33.CAR-CXCR4^{mut}-CIKs displayed consistently reduced CXCR4 downregulation after incubation with CXCL12 compared with the other CAR constructs ($n = 10$; $P < .0001$; supplemental Figure 3A-B). Accordingly, CXCL12-pretreated CD33.CAR-CXCR4^{mut}-CIKs ($n = 5$) mediated a superior chemotactic response to sequential stimulation in comparison with CD33.CAR-CXCR4^{wt}- ($P = .0068$) and CD33.CAR-CIKs ($P = .0020$; supplemental Figure 3C).

Overall, these data underline the relevance of the CXCL12 gradient generated within the BM in AML and the feasibility to genetically upregulate the CXCR4 on CD33.CAR-CIKs to promote their migration toward CXCL12.

CXCR4-overexpression on CD33.CAR-CIKs leads to enhanced chemotactic activity toward CXCL12 while retaining CAR-related effector functions

Next, we evaluated the chemotactic properties of CD33.CAR-CXCR4^{wt}- and CD33.CAR-CXCR4^{mut}-CIKs toward the CXCL12 gradient in a transwell migration assay. To determine the effective contribution of the engineered CXCR4^{wt} or CXCR4^{mut} molecules on CD33.CAR-CIK functionality, we selected CAR⁺-CIKs by immunomagnetic sorting (purity >99%; Figure 2A). Notably, both CD33.CAR⁺-CXCR4^{wt}- ($P = .015$) and CD33.CAR⁺-CXCR4^{mut}-CIKs ($P < .0001$) displayed improved migratory response toward rhCXCL12 compared with CD33.CAR-CIKs ($n = 10$). Specifically, CD33.CAR⁺-CIKs expressing CXCR4^{mut} migrated more efficiently than those expressing CXCR4^{wt} ($P = .0362$; Figure 2B). Afterward, to better mimic the conditions of the BM microenvironment, we used the supernatant of HD-MSCs or AML-MSCs as chemotactic

stimulus. No significant differences in CXCL12 levels were observed (Figure 2C). Remarkably, both CD33.CAR⁺-CXCR4^{wt}- and CD33.CAR⁺-CXCR4^{mut}-CIKs showed increased chemotactic response toward both HD-MSC and AML-MSC supernatants compared with control CD33.CAR⁺-CIKs ($n = 14$; $P < .0001$; Figure 2D). This enhanced migration is strictly associated with the presence of CXCL12 in the supernatant because it was abrogated after pretreatment with the CXCR4 antagonist plerixafor. Even in this case, CXCR4^{mut} promoted superior CXCL12-dependent chemotaxis compared with CXCR4^{wt} ($P = .0056$ for HD-MSC; and $P = .043$ for AML-MSC supernatants).

To assess whether CXCR4 overexpression may have an impact on CAR-related cytotoxic properties, we tested cytotoxicity, proliferation, and cytokine production of CD33.CAR⁺-CXCR4^{wt}- and CD33.CAR⁺-CXCR4^{mut}-CIKs incubated with the CD33⁺ KG-1 AML cell line and patient-derived primary AML cells, in the presence or absence of CXCL12.

CXCR4-overexpressing CD33.CAR⁺-CIKs retained specific cytotoxic activity against KG-1 cells and primary AML samples (Figure 2E). CD33.CAR⁺-CIKs overexpressing either CXCR4^{wt} or CXCR4^{mut} proliferated in response to CD33⁺ leukemic cells (Figure 2F). Moreover, the intracellular staining for IFN- γ and IL-2 revealed cytokine production after coculture with CD33⁺ target cells (Figure 2G). Of note, the presence of CXCL12 in the coculture enhanced the proliferation and the cytokine release of CD33.CAR⁺-CIKs expressing CXCR4^{mut}. The anti-leukemic activity of CD33.CAR⁺-CXCR4^{wt}-CIKs toward the KG-1 cell line and primary AML blasts was superior to that exerted by CD33.CAR-CIKs in the presence of CXCL12 at low effector to target (E:T) ratios (KG-1: $P = .03$ for E:T 0.25:1 and 0.125:1 [Figure 2H]; AML#1: $P = .016$ for E:T 0.125:1 [Figure 2I]). We then investigated the cytotoxic activity of CXCR4-overexpressing CD33.CAR-CIKs that migrated toward the CXCL12 gradient. The enhanced migration along the CXCL12 gradient resulted in significantly higher lysis of primary blasts by CXCR4^{wt}-overexpressing CD33.CAR⁺-CIKs compared with control CD33.CAR⁺-CIKs ($P = .002$; Figure 2L).

Overall, these data suggest that CXCR4 overexpression in CD33.CAR-CIKs increases their migration toward the CXCL12 gradient without compromising their cytotoxic activity against AML cell lines and primary blasts.

Figure 2 (continued) CD33.CAR⁺-CXCR4^{wt}- vs CD33.CAR⁺-CXCR4^{mut}-CIKs, using paired t test. (C) CXCL12 levels measured in the culture supernatant of BM-derived mesenchymal stromal cells from healthy donors (HD-MSCs, $n = 6$ different donors) or from pediatric patients with AML (AML-MSCs, $n = 10$ different donors). (D) Percentage of migration of CXCR4-overexpressing CD33.CAR⁺-CIKs in response to culture supernatant of HD-MSCs (left) or AML-MSCs (right) in the absence or presence of plerixafor (Plx). For HD-MSCs: $n = 12$ experiments using CAR-CIKs generated from 6 different donors and supernatant samples from 6 different HD-MSCs; **** $P < .0001$ and ** $P = .0056$, using paired t test. For AML-MSCs: $n = 14$ experiments using CAR-CIKs generated from 6 different donors and supernatant samples from 10 different AML-MSCs; **** $P < .0001$ and * $P = .043$, using paired t test. (E) Cytotoxicity (E:T ratio of 5:1) of CXCR4-overexpressing CD33.CAR⁺-CIKs against CD33⁺ KG-1 cell line and primary AML cells in the absence or presence of 200 ng/mL CXCL12 (for KG-1 with 200 ng/mL CXCL12: ** $P = .006$ using paired t test). (F) Proliferation of CXCR4-overexpressing CD33.CAR⁺-CIKs in response to CD33⁺ KG-1 cell line and primary AML cells in the absence or presence of 200 ng/mL CXCL12 (for AML#1 with 200 ng/mL CXCL12: * $P = .012$; ** $P = .003$; for AML#2 with 200 ng/mL CXCL12: * $P = .012$; for AML#3 with 200 ng/mL CXCL12: ** $P = .006$ for CD33.CAR⁺-CXCR4^{mut}- vs CD33.CAR⁺-CXCR4^{wt}-CIKs; ** $P = .002$ for CD33.CAR⁺-CXCR4^{mut}- vs CD33.CAR⁺-CIKs. A paired t test was used). (G) Cytokine release of CXCR4-overexpressing CD33.CAR⁺-CIKs in response to CD33⁺ KG-1 cell line and primary AML cells in the absence or presence of 200 ng/mL CXCL12 (IFN- γ : * $P = .012$; IL-2: for KG-1 with 200 ng/mL CXCL12, * $P = .029$; for AML#1 with 200 ng/mL CXCL12, * $P = .034$ and ** $P = .005$; for AML#2 and AML#3 with 200 ng/mL CXCL12, ** $P = .001$. A paired t test was used). For panels E, F, and G, $n = 9$ (for KG-1) and $n = 8$ (for primary AML cells) independent experiments using CAR-CIKs generated from different donors. (H-I) Quantification of (H) CD33⁺ KG-1 cell line and (I) primary AML cell lysis after 24 hours of coculture with CXCR4-overexpressing CD33.CAR⁺-CIKs at low E:T cell ratios, in the presence of 200 ng/mL CXCL12 (for KG-1 at E:T 0.25:1 and 0.125:1, * $P = .03$ for CD33.CAR⁺- vs CD33.CAR⁺-CXCR4^{wt}-CIKs; for AML#1 at E:T 0.125:1, * $P = .016$ for CD33.CAR⁺-CXCR4^{wt}- vs CD33.CAR⁺-CXCR4^{mut}-CIKs; and CD33.CAR⁺-CXCR4^{mut}-CIKs. A paired t test was used). $n = 5$ (for KG-1) and $n = 6$ (for AML#1) independent experiments using CAR-CIKs generated from different donors. (J) Cytotoxicity of CXCR4-overexpressing CD33.CAR⁺-CIKs after chemotaxis toward CXCL12 gradient. Migrated CIKs were harvested and cocultured for 4 hours with primary AML cells (for AML#1: ** $P = .002$ for CD33.CAR⁺-CXCR4^{wt}- vs CD33.CAR⁺-CIKs; * $P = .012$ for CD33.CAR⁺-CXCR4^{wt}- vs CD33.CAR⁺-CXCR4^{mut}-CIKs; for AML#2: ** $P = .002$ for CD33.CAR⁺-CXCR4^{wt}- vs CD33.CAR⁺-CIKs, ** $P = .009$ for CD33.CAR⁺-CXCR4^{wt}- vs CD33.CAR⁺-CXCR4^{mut}-CIKs. A paired t test was used). For each primary AML, $n = 8$ independent experiments using CAR-CIKs generated from 8 different donors.

CXCR4-overexpressing CD33.CAR-CIKs possess superior in vivo homing ability to the BM compared with control CD33.CAR-CIKs

To assess whether CXCR4-overexpressing CD33.CAR-CIKs acquire superior homing to the BM in vivo, we first established that CD33.CAR⁺-CXCR4^{wt}- and CD33.CAR⁺-CXCR4^{mut}-CIKs exhibit enhanced in vitro migration capacity in response to recombinant murine CXCL12 and mouse BM supernatant as compared with CD33.CAR⁺-CIKs (data not shown; Figure 3A). Afterward, NSG mice were infused IV with either CD33.CAR⁺-CXCR4^{wt}-, CD33.CAR⁺-CXCR4^{mut}-, or CD33.CAR⁺-CIKs (10⁷ cells per mouse; Figure 3B). The frequency and absolute number of hCD45⁺ cells recovered from the BM, PB, and spleen were determined via FACS analysis 7 days after transplant. The hCD45⁺ cell frequency was higher in the BM of mice that had received CD33.CAR⁺-CXCR4^{wt}-CIKs (n = 10) and CD33.CAR⁺-CXCR4^{mut}-CIKs (n = 12) compared with those infused with CD33.CAR⁺-CIKs (n = 12; *P* = .0038; and *P* = .0006; respectively; Figure 3C-D). Specifically, mice receiving CD33.CAR⁺-CXCR4^{mut}-CIKs showed the highest number of hCD45⁺ cells in the BM (vs CD33.CAR⁺-CIKs, *P* < .0001; vs CD33.CAR⁺-CXCR4^{wt}-CIKs, *P* = .0369) (Figure 3D). The frequency and the absolute number of CXCR4-overexpressing CD33.CAR⁺-CIKs in the PB and spleen displayed only minimal differences compared with control CD33.CAR⁺-CIKs (Figure 3E).

We then assessed the kinetics of CXCR4-overexpressing CD33.CAR⁺-CIKs in the niche by sampling the BM at days +10 and +14 after transplant. At day +10, mice treated with CD33.CAR⁺-CXCR4^{mut}-CIKs (n = 13) showed higher frequency and number of hCD45⁺ cells in the BM compared with those treated with CD33.CAR⁺-CIKs (n = 12; *P* < .0001; Figure 3F). These results were further confirmed on day +14 because CD33.CAR⁺-CXCR4^{mut}-CIKs (n = 10) were still present in the BM compartment at higher levels than were CD33.CAR⁺-CIKs (n = 11; *P* < .0001; Figure 3G).

Overall, these data suggest that CXCR4 overexpression on CD33.CAR-CIKs increases their migration to the BM and, in the case of the mutated CXCR4, further prolongs their persistence.

CXCR4^{wt}-overexpressing CD33.CAR-CIKs promote better elimination of BM-resident AML cells and prolong the survival of mice

To verify whether CXCR4-overexpression in CD33.CAR-CIKs confers superior antitumor activity, we established a leukemia xenograft model by injecting hCD33⁺ KG-1 cells into NSG mice. Fourteen days later, mice were treated with CD33.CAR⁺-CXCR4^{wt}-, CD33.CAR⁺-CXCR4^{mut}-, or control CD33.CAR⁺-CIKs. In the first set of experiments, mice were euthanized 25 days after CAR-CIK infusion and the frequency of residual hCD33⁺ cells in the BM, PB, and spleen was monitored via FACS analysis (Figure 4A). Animals treated with CD33.CAR⁺-CIKs displayed a reduction in the frequency and absolute number of hCD33⁺ cells in the BM. The treatment with CXCR4-overexpressing CD33.CAR⁺-CIKs further decreased the amount of hCD33⁺ KG-1 cells, specifically in the case of CD33.CAR⁺-CXCR4^{wt}-CIKs (percentage: vs CD33.CAR⁺-CIKs [*P* = .0106], vs CD33.CAR⁺-CXCR4^{mut}-CIKs [*P* = .0336]; absolute number: vs CD33.CAR⁺-CIKs [*P* = .0156], vs CD33.CAR⁺-CXCR4^{mut}-CIKs [*P* = .0418]; Figure 4B-C). Similarly, immunohistochemistry

analyses showed that hCD33⁺ AML cells were almost undetectable in the BM of the CD33.CAR⁺-CXCR4^{wt}-CIK-treated group (supplemental Figure 4). Moreover, reduction of leukemic burden was observed in the spleen, in which CXCR4-overexpressing CD33.CAR⁺-CIKs showed enhanced antitumor activity compared with CD33.CAR⁺-CIKs (percentage: *P* = .0003 for CD33.CAR⁺-CXCR4^{wt}-CIKs and *P* = .0086 for CD33.CAR⁺-CXCR4^{mut}-CIKs; absolute number: *P* = .00107 for CD33.CAR⁺-CXCR4^{wt}-CIKs and *P* = .033 for CD33.CAR⁺-CXCR4^{mut}-CIKs [Figure 4D]). Similarly, low hCD33⁺ AML residual cells were detected in the PB of mice treated with CXCR4-overexpressing CD33.CAR⁺-CIKs and control CD33.CAR⁺-CIKs (Figure 4D). We did not observe any accumulation of CD33.CAR⁺-CXCR4^{wt}- and CD33.CAR⁺-CXCR4^{mut}-CIKs in tissues expressing CXCL12 (ie, liver, heart, kidney, and brain) after IV administration. Moreover, there were no obvious signs of histological damage in these organs (data not shown).

In the second set of experiments, leukemia burden was monitored weekly in BM aspirates, starting from 2 weeks after CAR-CIK infusion, and mice survival was evaluated (Figure 4E). By week 7, CD33.CAR⁺-CXCR4^{wt}-CIKs demonstrated a superior control of AML progression with lower amounts of AML cells in the BM compared with CD33.CAR⁺-CXCR4^{mut}- and CD33.CAR⁺-CIK groups (n = 4 mice per group; Figure 4F). In association with the reduced leukemic tumor burden, the survival of the KG-1 cell-inoculated mice treated with CD33.CAR⁺-CXCR4^{wt}-CIKs was significantly prolonged (n = 4 mice per group; *P* = .0001; log-rank test), with the median survival time increased from 57.5, 77.5, and 87.5 days in the untreated, CD33.CAR⁺-CIK, and CD33.CAR⁺-CXCR4^{mut}-CIK groups, respectively, to 110 days in the CD33.CAR⁺-CXCR4^{wt}-CIK group (vs CD33.CAR⁺-CIKs [*P* = .010], vs CD33.CAR⁺-CXCR4^{mut}-CIKs [*P* = .010]; Figure 4G). The unexpected underperformance of CD33.CAR⁺-CXCR4^{mut}-CIKs could be ascribed to immunological synapse instability. In fact, it was reported that in the presence of competing CXCL12 signal the stability of the immune synapse of T lymphocytes from patients with WHIM-mutant CXCR4 is disrupted as a result of impaired recruitment of the mutant receptor.²³ Hence, we performed conjugate stability experiments in which CD33.CAR⁺-CXCR4^{wt}- and CD33.CAR⁺-CXCR4^{mut}-CIKs were brought into contact with labeled CD33⁺ or CD33⁻ KG-1 cells to form conjugates. When exposed to CXCL12, CD33.CAR⁺-CXCR4^{wt}-CIKs conjugated with CD33⁺ KG-1 were less responsive and migrated less efficiently than unengaged CD33.CAR⁺-CXCR4^{wt}-CIKs left in contact with CD33⁻ KG-1 cells. In contrast, CD33.CAR⁺-CXCR4^{mut}-CIKs conjugated with CD33⁺ KG-1 were still efficiently attracted and migrated toward the chemokine, suggesting an impaired conjugate stability in the presence of competing external CXCL12 signals (*P* = .00058 for CD33.CAR⁺-CXCR4^{mut}-CIKs vs CD33.CAR⁺-CXCR4^{wt}-CIKs; Figure 4H).

Overall, these findings demonstrate that CXCR4^{wt} overexpression in CD33.CAR-CIKs favorably improves the antileukemic effect of these cells.

Discussion

We have developed a novel approach to engineer CIKs to coexpress CD33.CAR and CXCR4, in both wt and WHIM syndrome-derived truncated forms. Both of these engineered

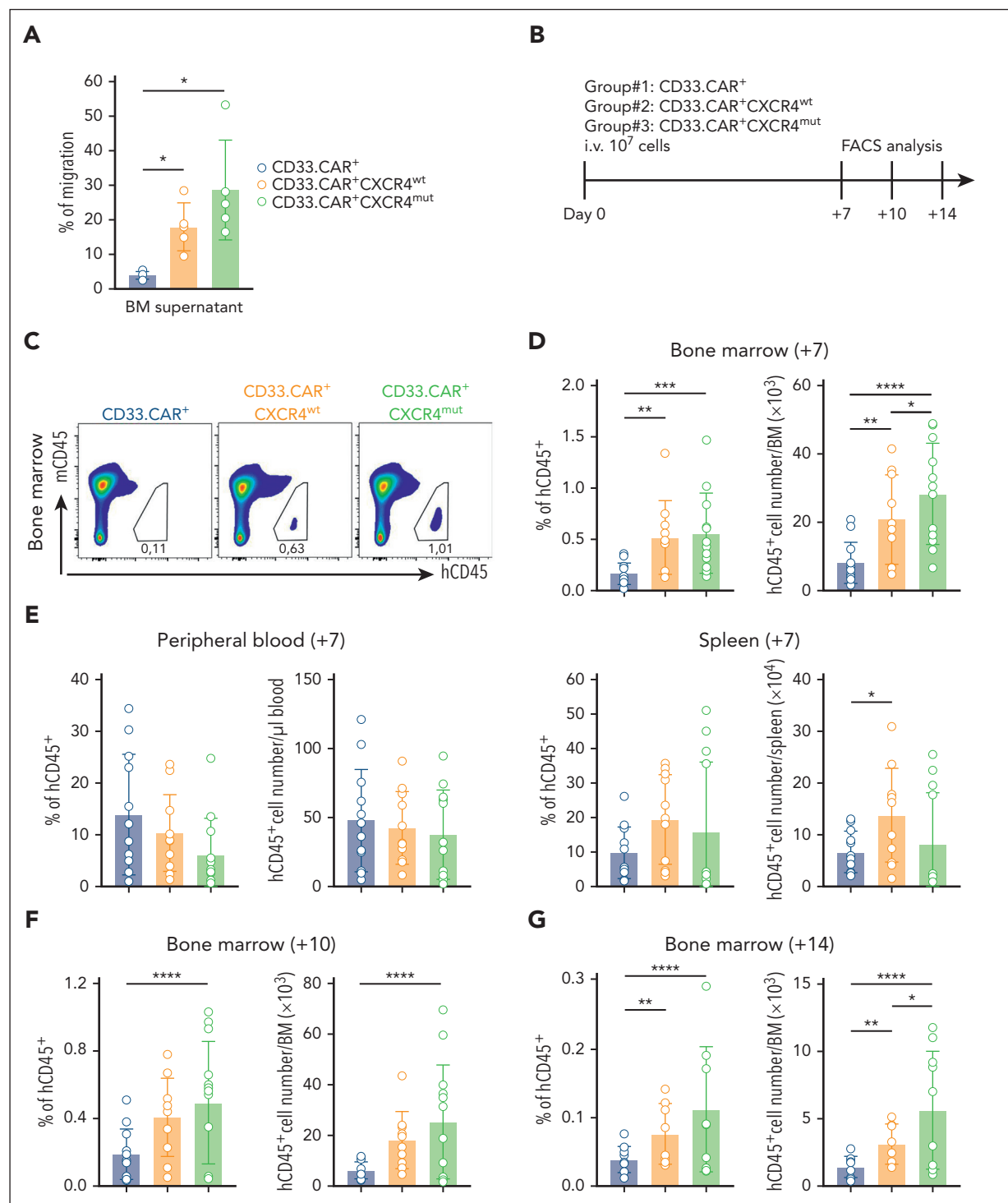


Figure 3. CXCR4-overexpressing CD33.CAR-CIKs have enhanced in vivo BM homing ability. Data are presented as individual values and the mean ± SD. (A) Percentage of migration of CXCR4-overexpressing CD33.CAR⁺-CIKs in response to mouse BM supernatant (n = 5 independent experiments using CAR-CIKs generated from 1 donor and supernatant samples from 5 different mice; *P = .027 using paired t test). (B) Scheme of CD33.CAR-CIKs homing model using NSG mice inoculated via tail vein injection with 10⁷ CD33.CAR⁺-, CD33.CAR⁺-CXCR4^{wt}-, or CD33.CAR⁺-CXCR4^{mut}-CIKs. Mice were euthanized 7, 10, or 14 days after infusion, and hCD45⁺CD3⁺ T cells were enumerated in the BM, PB, and spleen via flow cytometry. (C) Representative flow cytometry plots of hCD45⁺ cell engraftment within mice BM at 7 days after infusion. (D-E) Summary of the percentages and absolute numbers of hCD45⁺ in (D) the BM, and (E) the PB and spleen of mice at 7 days after infusion (n = 12 mice in the CD33.CAR⁺- and CD33.CAR⁺-CXCR4^{mut}-CIKs groups, n = 11 mice in the CD33.CAR⁺-CXCR4^{wt}-CIKs group. Three independent experiments using CAR-CIKs generated from 3 different donors. For percentage of hCD45⁺ in the BM: ***P = .0006 and **P = .0038. For the absolute number of hCD45⁺ in the BM: ****P < .0001, **P = .0035, and *P = .0369. For the absolute number of hCD45⁺ in the spleen: *P = .0393. A mixed-effect model was used). (F-G) Summary of the percentages and absolute numbers of hCD45⁺ in the BM of mice euthanized 10 days (F) or 14 days (G) after infusion (n = 12 mice in the CD33.CAR⁺-CIKs group, n = 10 mice in the CD33.CAR⁺-CXCR4^{wt}-CIKs group, and n = 13 mice in the CD33.CAR⁺-CXCR4^{mut}-CIKs group for experiments at 10 days; ****P < .0001. n = 11 mice in the CD33.CAR⁺-CIKs group, n = 8 mice in the CD33.CAR⁺-CXCR4^{wt}-CIKs group, and n = 10 mice in the CD33.CAR⁺-CXCR4^{mut}-CIKs group for experiments at 14 days; ****P < .0001, **P = .0029, and *P = .0425. Three independent experiments using CAR-CIKs generated from 3 different donors. A mixed-effect model was used).

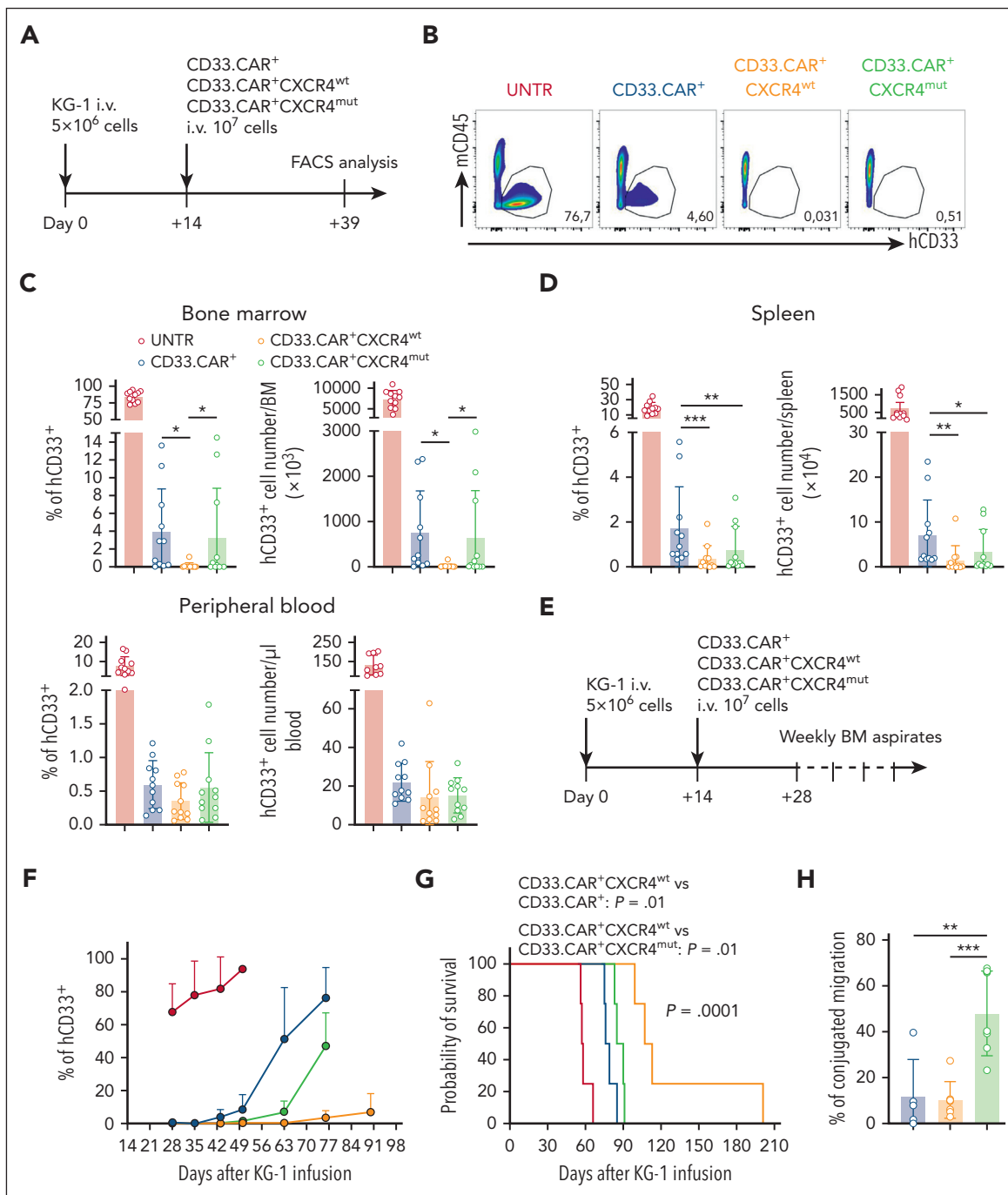


Figure 4. CXCR4^{wt}-overexpressing CD33.CAR-CIKs have superior antileukemic activity against KG-1 cells in the BM. Data are shown as mean values \pm SD. (A) Scheme of the AML model using NSG mice inoculated, via tail vein injection, with 5×10^6 KG-1 cells and 14 days later with CD33.CAR⁺, CD33.CAR⁺CXCR4^{wt}, or CD33.CAR⁺CXCR4^{mut}-CIKs (10⁷ cells per mouse). Mice were euthanized 25 days after CD33.CAR-CIKs infusion and hCD45⁺CD33⁺ leukemia cells were enumerated in the BM, PB, and spleen via flow cytometry. (B) Representative flow cytometry plots of hCD33⁺ cell engraftment in the BM of mice untreated (UNTR) or treated. (C-D) Summary of the percentages and absolute numbers of hCD33⁺ in (C) the BM (for percentage: *P = .0106 for CD33.CAR⁺ vs CD33.CAR⁺CXCR4^{wt}-CIKs; and *P = .0336 for CD33.CAR⁺CXCR4^{wt} vs CD33.CAR⁺CXCR4^{mut}-CIKs; for absolute number: *P = .0156 for CD33.CAR⁺ vs CD33.CAR⁺CXCR4^{wt}-CIKs; and *P = .0418 for CD33.CAR⁺CXCR4^{wt} vs CD33.CAR⁺CXCR4^{mut}-CIKs, using a mixed-effect model), and (D) the spleen and PB (for percentage in the spleen: ***P = .0003 and **P = .0086; for absolute number in the spleen: **P = .00107 and *P = .033, using a mixed-effect model), of mice at 25 days (n = 11 mice per group). Three independent experiments using CAR-CIKs generated from 3 different donors. (E) In a second experimental setting, using the same model shown in panel B, femoral BM aspiration was performed on mice starting from day 14 after CD33.CAR-CIK injection until survival, and percentage of hCD33⁺ leukemia cells in the BM was analyzed via flow cytometry. (F) Summary of percentage of hCD33⁺ cells in the BM, n = 4 mice per group from 4 independent experiments using CAR-CIKs generated from 4 different donors. (G) Kaplan-Meier survival curves of the same mice in panel F. Comparisons of survival curves were determined using log-rank test. (H) Percentage of residual migration of conjugates formed by CD33.CAR⁺, CD33.CAR⁺CXCR4^{wt}, or CD33.CAR⁺CXCR4^{mut}-CIKs with CD33⁺ KG-1 (stable conjugates) relative to CD33⁻ KG-1 cells (control). The conjugates were allowed to migrate toward CXCL12 in a transwell filter allowing the migration of single cells only (n = 7 independent experiments using CAR-CIKs generated from 7 different donors; ***P = .0006 and **P = .00101, using t test).

CXCR4-overexpressing CD33.CAR-ClCs displayed increased migration toward the chemokine CXCL12 and effectively killed CD33⁺ cell lines and primary AML cells. However, although CAR-ClCs engineered with the CXCR4^{mut} variant demonstrated a prolonged retention in the BM compared with CAR-ClCs coexpressing CXCR4^{wt}, the latter led to superior disease control, emphasizing that the physiological modulation of CXCR4 in ClCs may have an essential role in modulating both their accrual and release from the leukemic BM niche as well as their activation status.

Strategies to improve CAR T-cell recruitment to the tumor have recently raised interest not only in solid tumors but also in hematological malignancies. Specifically, in AML, in which the efficacy of CAR T-cell therapy is hampered, the homing of blood-injected effector cells to the BM is required for their intimate contact with BM-residing leukemia cells, including LSCs, whose elimination is fundamental to achieve deep and durable remission.

In particular, we explored the possibility to exploit the CXCL12/CXCR4 axis, which is critical in the AML niche, in order to maximize CD33.CAR-ClC recruitment to the BM, thus possibly increasing their therapeutic efficacy. The CXCR4 receptor is involved in the homing of hematopoietic and immune cells into the BM niche, and therefore can be leveraged to drive CAR T cells into the niche in response to the CXCR4 ligand, CXCL12, produced by multiple cell types, such as stromal cells, endothelial cells, and osteoblasts.²⁴ In a previous study, CXCR4 was coexpressed on c-kit CAR T cells to maximize the hematopoietic stem cell clearance within the BM.²⁵ Furthermore, CXCR4 upregulation on anti-EpCAM.CAR T cells, obtained by ex vivo treatment with rapamycin, has shown increased BM infiltration and elimination of marrow-resident AML cells in a xenograft mouse model.⁴

The CXCL12/CXCR4 axis is central to AML pathogenesis because it controls blast adhesion into the protective BM niche, adaptation to the hypoxic environment, and cellular migration and survival.¹⁰ High levels of CXCR4 expression in blasts are associated with poor relapse-free and overall survival.²⁶ Furthermore, blocking the CXCL12/CXCR4 axis is an attractive therapeutic strategy because it can lead to the mobilization of AML cells from the BM into the circulation, depriving them of essential survival signals.¹⁰⁻¹² Moreover CXCL12/CXCR4 is implicated in the homing of regulatory T cells to the BM microenvironment in AML.^{27,28}

To enhance migration and also increase CAR-ClC retention in the BM, bringing them in closer contact with BM-residing LSCs, we also postulated the use of GOF variants of CXCR4. GOF mutations of CXCR4, with the most prevalent being the R334X mutant, are a cause of WHIM syndrome, which results in pancytopenia in the PB and hyperplasia in the BM.¹⁴ This is likely caused by the stronger binding of the carboxyl-terminal-truncated WHIM CXCR4 mutant to CXCL12, increasing intracellular signaling and preventing release of leukocytes into the PB from the BM.¹⁵ Levy et al showed that transfecting NK cells with GOF mutant variant of CXCR4 leads to superior BM homing.²⁹ In addition, CXCR4^{R334X} reportedly is effective in enhancing the controlling effects of anti-B-cell maturation antigen (BCMA) CAR-NK cells have on in vivo multiple myeloma growth.³⁰

In our study, we observed that CXCR4 is strongly downregulated in CD33.CAR-ClCs during ex vivo expansion and demonstrated that CXCR4 expression can be stably increased in CD33.CAR-ClCs using a bicistronic SB transposon vector containing 2A-like peptide, without negatively affecting their phenotype.

Compared with CD33.CAR⁺-ClCs, both CD33.CAR⁺-CXCR4^{wt}- and CD33.CAR⁺-CXCR4^{mut}-ClCs showed improved chemotaxis toward rhCXCL12 or HD/AML-MS supernatants. Using CD33⁺ AML cell lines as well as primary AML cells as the target, similar cytotoxic activity, proliferative response, and IFN- γ or IL-2 secretion levels were observed in CD33.CAR⁺-ClCs, regardless of whether they overexpressed CXCR4^{wt}, CXCR4^{mut}, or none.

Finally, our data establish the feasibility and efficacy of a single administration of CXCR4-overexpressing CD33.CAR⁺-ClCs to control leukemia in vivo in a xenograft model. First, both the CXCR4-engineered products displayed enhanced in vivo BM homing, along with prolonged BM retention in the case of CXCR4^{mut}, as expected. However, only CD33.CAR⁺-ClCs coexpressing CXCR4^{wt} exerted a superior control of AML progression when compared with the conventional CD33.CAR⁺-ClCs, significantly increasing the survival time of treated mice.

In addition to the enhanced BM homing, the increased antileukemic effects of CD33.CAR-CXCR4^{wt}-ClCs could be determined by other factors. CXCR4 is known to affect T-cell costimulation because CXCL12 facilitates the formation of the immunological synapse and amplifies the downstream T-cell receptor intracellular signaling.^{31,32} This mechanism could explain, at least in part, our experimental observation that CXCL12 increases the cytotoxic effects of CD33.CAR-CXCR4^{wt}-ClCs at lower E:T ratios. In contrast, we found that CD33.CAR-CXCR4^{mut}-ClCs have reduced antileukemic effects in vivo, which resembles the effects of the WHIM-mutant CXCR4 that delivers aberrant signals to T and B cells. Firstly, in the presence of distracting CXCL12, CXCR4 mutant competes with the T-cell receptor signaling, therefore disrupting T-cell-antigen presenting cell synapses, thus inhibiting T-cell activation rather than enhancing it.²³ Consistently, we confirmed that CXCR4^{mut} disrupts the stability of CD33.CAR⁺-ClCs/target-cell conjugates in vitro, and this may dampen CAR-ClCs activation and their downstream effector functions. Furthermore, it was reported that WHIM-mutant CXCR4, because of its impaired CXCL12-induced downregulation, may lead to aberrant T-cell hyperactivation in response to CXCL12, reducing their survival.³³ Interestingly, in the presence of CXCL12, CD33.CAR-CXCR4^{mut}-ClCs have shown in vitro increased proliferation and cytokine production in response to AML cells. Therefore, this hyperactivation mediated by CXCL12-stimulated WHIM-mutant CXCR4 coupled with the CAR signaling can lead in vivo to activation-induced cell death and CAR-ClC exhaustion, reducing their persistence. In contrast to our data, Ng et al reported that CXCR4^{R334X}-modified anti-BCMA CAR-NK cells have improved control of multiple myeloma in the BM.³⁰ However, they electroporated the effector cells with a CXCR4^{R334X}-encoding messenger RNA, obtaining an only transient expression of the receptor (<48 hours), thus avoiding the potential effects of CXCL12-mediated aberrant costimulation in vivo.

Regarding the potential off-target effects of this CXCR4-mediated approach, a GTEx database analysis of expression levels of CXCL12 showed its expression on healthy tissues other than the BM, such as heart, liver, kidney, and brain, and thus we cannot

fully exclude potential side effects in patients. In our studies we did not observe any evidence of accumulation of CXCR4-modified CD33.CAR-CIKs in healthy tissues, and we did not record side effects in animals within the limitations of the xenograft model. We used CD33 as the target for our studies, as a proof-of-principle, based on the previous preclinical experience with CAR T cells for AML.^{13,34-37} However, CD33 may cause on-target off-tumor toxicity in healthy hematopoietic stem and progenitor cells. However, the concept of coupling CAR and CXCR4 expression in T cells to increase their BM homing remains broadly applicable to other AML-associated antigens.

In conclusion, to our knowledge, this study provides a proof-of-concept that demonstrates that arming anti-AML CAR-CIKs with the CXCR4^{wt} is a feasible strategy to enhance control of the AML burden in the BM niche, showing striking efficacy in vitro and in vivo.

Acknowledgments

The authors thank M. Kallikourdis for the helpful discussion and suggestions regarding the CXCR4^{mut} and M. Cereda for the GTEX database analysis on expression levels of CXCL12 in organs. They also thank the parent committees Comitato Maria Letizia Verga, Quelli che...con Luca Onlus, and Amici di Duccio for their generous and constant support.

This work was supported by grants from AIRC 5 × 1000 Immunity in Cancer Spreading and Metastasis (grant 21147), AIRC IG 2022 (grant 27507), AIRC IG 2018 (grant 22082), and the Ministero della Salute Research project on CAR T cells for hematological malignancies and solid tumors conducted under the aegis of Alliance Against Cancer network, and PRIN 2021-NAZ-0033.

Authorship

Contribution: M.B., G.D., A.P., and M.S. supervised the study and wrote the manuscript; M.B., S.T., G.D., A.P., and M.S. determined the methodology; M.B., B.C., C.T., S.D., S.B., V.M.P., A.D., and A.P. performed the investigation; M.B., S.D., S.B., A.D., and A.P. curated the data; M.B., S.G., and A.P. formally analyzed the data; S.G. performed statistical analysis; R.P. performed gene expression analyses; S.T., V.B., F.D., A.M., and A.B. critically discussed data and edited the manuscript; A.B. and M.S. provided the funding; and F.D., G.D., A.P., and M.S. conceived the study.

Conflict-of-interest disclosure: G.D. served as a consultant for Bellicum Pharmaceuticals and Catamaran. The remaining authors declare no competing financial interests.

The current affiliation for F.D. is AstraZeneca, Cambridge, United Kingdom.

ORCID profiles: M.B., 0000-0003-1156-2255; S.T., 0000-0002-7327-418X; S.G., 0000-0003-1504-7242; C.T., 0000-0002-6576-5042; R.P., 0000-0003-4198-9620; S.D., 0000-0001-6970-758X; S.B., 0000-0003-3561-9113; V.M.P., 0000-0003-4105-9087; V.B., 0000-0003-4050-0926; A.D., 0000-0001-9203-5814; F.D., 0000-0003-2407-236X; A.M., 0000-0001-5578-236X; A.B., 0000-0002-6757-6173; A.P., 0000-0002-6189-1885; M.S., 0000-0001-8105-6476.

Correspondence: Marta Serafini, Tettamanti Center, Fondazione IRCCS San Gerardo dei Tintori, Via Pergolesi 33, 20900 Monza, Italy; email: serafinim72@gmail.com; and Andrea Biondi, Pediatrics, Fondazione IRCCS San Gerardo dei Tintori, Via Pergolesi 33, 20900 Monza, Italy; email: abiondi.unimib@gmail.com.

Footnotes

Submitted 9 September 2022; accepted 3 February 2023; prepublished online on *Blood* First Edition 14 February 2023. <https://doi.org/10.1182/blood.2022018330>.

*A.P. and M.S. contributed equally to this study

The data reported in this article have been deposited in the Gene Expression Omnibus database (accession numbers GSE214914 and GSE128423) and The European Genome-phenome Archive (accession number EGAS00001005593).

EGAS00001005593 data can be interactively explored using a dedicated Abseq App (<https://abseqapp.shiny.embl.de/>).

The data generated in this study are available within the article and its supplemental data files.

The online version of this article contains a data supplement.

There is a *Blood* Commentary on this article in this issue.

The publication costs of this article were defrayed in part by page charge payment. Therefore, and solely to indicate this fact, this article is hereby marked "advertisement" in accordance with 18 USC section 1734.

REFERENCES

- Mardiana S, Gill S. CAR T cells for acute myeloid leukemia: state of the art and future directions. *Front Oncol*. 2020;10:697.
- Ritchie DS, Neeson PJ, Khot A, et al. Persistence and efficacy of second-generation CAR T cell against the leu antigen in acute myeloid leukemia. *Mol Ther*. 2013; 21(11):2122-2129.
- Zou Y, Li F, Hou W, Sampath P, Zhang Y, Thorne SH. Manipulating the expression of chemokine receptors enhances delivery and activity of cytokine-induced killer cells. *Br J Cancer*. 2014;110(8):1992-1999.
- Nian Z, Zheng X, Dou Y, et al. Rapamycin pretreatment rescues the bone marrow AML cell elimination capacity of CAR-T cells. *Clin Cancer Res*. 2021;27(21):6026-6038.
- Di Stasi A, De Angelis B, Rooney CM, et al. T lymphocytes coexpressing CCR4 and a chimeric antigen receptor targeting CD30 have improved homing and antitumor activity in a Hodgkin tumor model. *Blood*. 2009; 113(25):6392-6402.
- Craddock JA, Lu A, Bear A, et al. Enhanced tumor trafficking of GD2 chimeric antigen receptor T cells by expression of the chemokine receptor CCR2b. *J Immunother*. 2010;33(8):780-788.
- Moon EK, Carpenito C, Sun J, et al. Expression of a functional CCR2 receptor enhances tumor localization and tumor eradication by retargeted human t cells expressing a mesothelin-specific chimeric antibody receptor. *Clin Cancer Res*. 2011; 17(14):4719-4730.
- Lesch S, Blumenberg V, Stoiber S, et al. T cells armed with C-X-C chemokine receptor type 6 enhance adoptive cell therapy for pancreatic tumours. *Nat Biomed Eng*. 2021; 5(11):1246-1260.
- Cadilha BL, Benmebarek MR, Dorman K, et al. Combined tumor-directed recruitment and protection from immune suppression enable CAR T cell efficacy in solid tumors. *Sci Adv*. 2021;7(24):1-12.
- Ladikou EE, Chevassut T, Pepper CJ, Pepper AGS. Dissecting the role of the CXCL12/CXCR4 axis in acute myeloid leukaemia. *Br J Haematol*. 2020;189(5):815-825.
- Nervi B, Ramirez P, Rettig MP, et al. Chemosensitization of acute myeloid leukemia (AML) following mobilization by the CXCR4 antagonist AMD3100. *Blood*. 2009; 113(24):6206-6214.
- Uy GL, Rettig MP, Motabi IH, et al. A phase 1/2 study of chemosensitization with the CXCR4 antagonist plerixafor in relapsed or refractory acute myeloid leukemia. *Blood*. 2012;119(17):3917-3924.
- Rotiroti MC, Buracchi C, Arcangeli S, et al. Targeting CD33 in chemoresistant AML

- patient-derived xenografts by CAR-CIK cells modified with an improved SB transposon system. *Mol Ther*. 2020;28(9):1974-1986.
14. McDermott DH, Murphy PM. WHIM syndrome: immunopathogenesis, treatment and cure strategies. *Immunol Rev*. 2019; 287(1):91-102.
 15. Balabanian K, Lagane B, Pablos JL, et al. WHIM syndromes with different genetic anomalies are accounted for by impaired CXCR4 desensitization to CXCL12. *Blood*. 2005;105(6):2449-2457.
 16. Magnani CF, Turazzi N, Benedicenti F, et al. Immunotherapy of acute leukemia by chimeric antigen receptor-modified lymphocytes using an improved Sleeping Beauty transposon platform. *Oncotarget*. 2016;7(32):51581-51597.
 17. Triana S, Vonficht D, Jopp-Saile L, et al. Single-cell proteo-genomic reference maps of the hematopoietic system enable the purification and massive profiling of precisely defined cell states. *Nat Immunol*. 2021; 22(12):1577-1589.
 18. Baryawno N, Przybylski D, Kowalczyk MS, et al. A cellular taxonomy of the bone marrow stroma in homeostasis and leukemia. *Cell*. 2019;177(7):1915-1932.e16.
 19. Beider K, Nagler A, Wald O, et al. Involvement of CXCR4 and IL-2 in the homing and retention of human NK and NK T cells to the bone marrow and spleen of NOD/SCID mice. *Blood*. 2003;102(6): 1951-1958.
 20. Gulino AV, Moratto D, Sozzani S, et al. Altered leukocyte response to CXCL12 in patients with warts hypogammaglobulinemia, infections, myelokathexis (WHIM) syndrome. *Blood*. 2004;104(2):444-452.
 21. Hernandez PA, Gorlin RJ, Lukens JN, et al. Mutations in the chemokine receptor gene CXCR4 are associated with WHIM syndrome, a combined immunodeficiency disease. *Nat Genet*. 2003;34(1):70-74.
 22. Kawai T, Choi U, Whiting-Theobald NL, et al. Enhanced function with decreased internalization of carboxy-terminus truncated CXCR4 responsible for WHIM syndrome. *Exp Hematol*. 2005;33(4):460-468.
 23. Kallikourdis M, Trovato AE, Anselmi F, et al. The CXCR4 mutations in WHIM syndrome impair the stability of the T-cell immunologic synapse. *Blood*. 2013;122(5):666-673.
 24. Sugiyama T, Kohara H, Noda M, Nagasawa T. Maintenance of the hematopoietic stem cell pool by CXCL12-CXCR4 chemokine signaling in bone marrow stromal cell niches. *Immunity*. 2006;25(6):977-988.
 25. Arai Y, Choi U, Corsino CI, et al. Myeloid conditioning with c-kit-targeted car-t cells enables donor stem cell engraftment. *Mol Ther*. 2018;26(5):1181-1197.
 26. Spoo AC, Lübbert M, Wierda WG, Burger JA. CXCR4 is a prognostic marker in acute myelogenous leukemia. *Blood*. 2007;109(2): 786-791.
 27. Zou L, Barnett B, Safah H, et al. Bone marrow is a reservoir for CD4+CD25+ regulatory T cells that traffic through CXCL12/CXCR4 signals. *Cancer Res*. 2004;64(22):8451-8455.
 28. Wang R, Feng W, Wang H, et al. Blocking migration of regulatory T cells to leukemic hematopoietic microenvironment delays disease progression in mouse leukemia model. *Cancer Lett*. 2020;469:151-161.
 29. Levy E, Reger R, Segerberg F, et al. Enhanced bone marrow homing of natural killer cells following mRNA transfection with gain-of-function variant CXCR4R334X. *Front Immunol*. 2019;10:1262.
 30. Ng YY, Du Z, Zhang X, Chng WJ, Wang S. CXCR4 and anti-BCMA CAR co-modified natural killer cells suppress multiple myeloma progression in a xenograft mouse model. *Cancer Gene Ther*. 2022;29(5):475-483.
 31. Molon B, Gri G, Bettella M, et al. T cell costimulation by chemokine receptors. *Nat Immunol*. 2005;6(5):465-471.
 32. Kumar A, Humphreys TD, Kremer KN, et al. CXCR4 physically associates with the T cell receptor to signal in T cells. *Immunity*. 2006; 25(2):213-224.
 33. Roselli G, Martini E, Lougaris V, Badolato R, Viola A, Kallikourdis M. CXCL12 mediates aberrant costimulation of B lymphocytes in warts, hypogammaglobulinemia, infections, myelokathexis immunodeficiency. *Front Immunol*. 2017;8:1068.
 34. Marin V, Pizzitola I, Agostoni V, et al. Cytokine-induced killer cells for cell therapy of acute myeloid leukemia: improvement of their immune activity by expression of CD33-specific chimeric receptors. *Haematologica*. 2010;95(12):2144-2152.
 35. Pizzitola I, Anjos-Afonso F, Rouault-Pierre K, et al. Chimeric antigen receptors against CD33/CD123 antigens efficiently target primary acute myeloid leukemia cells in vivo. *Leukemia*. 2014;28(8): 1596-1605.
 36. Dutour A, Marin V, Pizzitola I, et al. In vitro and in vivo antitumor effect of anti-CD33 chimeric receptor-expressing EBV-CTL against CD 33 + acute myeloid leukemia. *Adv Hematol*. 2012;2012:683065.
 37. O'Hear C, Heiber JF, Schubert I, Fey G, Geiger TL. Anti-CD33 chimeric antigen receptor targeting of acute myeloid leukemia. *Haematologica*. 2015;100(3):336-344.

© 2023 by The American Society of Hematology.
Licensed under Creative Commons Attribution-NonCommercial-NoDerivatives 4.0 International (CC BY-NC-ND 4.0), permitting only noncommercial, nonderivative use with attribution. All other rights reserved.